



Atazanavir-Loaded Crosslinked Gamma-Cyclodextrin Nanoparticles to Improve Solubility and Dissolution Characteristics

✉ Darshana DHABLIYA, ✉ Shagufta Abdul Qaiyum KHAN*, ✉ Minal UMATE, ✉ Bhavana RAUT, ✉ Dilesh SINGHAVI

Institute of Pharmaceutical Education and Research, Maharashtra, India

ABSTRACT

Objectives: Atazanavir sulfate (AS), a Biosafety Cabinet (BCS) class II antiretroviral drug, shows dissolution rate-limited bioavailability, therefore, it is necessary to improve its solubility and oral bioavailability. The present investigation is intended to improve the aqueous solubility by developing AS-loaded nanoparticles (ASNPs). Additionally, the immediate release formulation of AS capsules has gastrointestinal side effects such as nausea and abdominal pain, cardiovascular side effect, *e.g.* abnormal cardiac conduction, toxic effects on kidney and liver such as nephrolithiasis, hyperbilirubinemia, and jaundice. Therefore, ASNPs were designed to release the drug slowly for 12 h, so that these side effects could be reduced.

Materials and Methods: ASNPs were prepared using gamma-cyclodextrin (γ -CD) and the crosslinker dimethyl carbonate were characterized by differential scanning calorimetry (DSC) and X-ray diffraction (XRD) to check the crystal characteristics of AS upon entrapment in NPs. Entrapment efficiency (EE), particle size, morphology, solubility, and dissolution behavior were also determined.

Results: EE%, particle size, and zeta potential varied from 14.38 ± 0.16 to $75.97 \pm 0.28\%$, 65.4 ± 1.25 nm to 439.6 ± 2.21 nm, and 28.3 ± 0.1 mV to 41.0 ± 0.3 mV, respectively. XRD and DSC confirmed the transformation of the crystalline AS to amorphous in NPs. There was 11.717 folds rise in AS solubility in water from NPs. The formulation having AS: γ -CD, 1:1 at 10 mg/mL, depicted 88.55 ± 0.58 , 91.23 ± 0.80 , and $86.8 \pm 0.65\%$ drug release in water, acid buffer, and phosphate buffer, respectively, in 12 h.

Conclusion: Solubility enhancement could be attributed to the decrease in crystallinity of atazanavir, when dispersed in NPs.

Key words: Atazanavir sulfate, gamma-cyclodextrin, nanoparticle solubility, dissolution behavior

INTRODUCTION

The poor solubility of potent therapeutics is a major concern in the development of their effective dosage forms because they show dissolution rate-limited bioavailability. One of the challenging tasks in the drug development process of such drugs is to improve the aqueous solubility in order to enhance their bioavailability. The bioavailability of Biosafety Cabinet (BCS) II drugs may be enhanced by increasing solubility and dissolution rate of the drug in the gastrointestinal fluid, as for rate-limiting step is drug release from the dosage form and solubility in the gastric fluid and not the absorption; so increasing the solubility will consequently improve the bioavailability.¹⁻³

The important techniques that increase the oral bioavailability of drugs with low aqueous solubility include micronization, nanosizing, co-crystallization, solid-lipid nanoparticles (SLNs), microemulsion, self-emulsifying drug delivery system, self-microemulsifying drug delivery systems, and liposomes.^{4,5} The saquinavir-loaded poly(alkylcyanoacrylate)/HP β CD nanoparticles (NP) prepared by Boudad et al.⁶ increased apparent solubility of saquinavir by 400 folds compared with free saquinavir. Sawant et al.⁷ have studied *in vitro* and *ex vivo* characteristics of valsartan-loaded SLNs. They reported improvement in the bioavailability of valsartan and suggested that SLNs can bypass the first-pass metabolism, enhance

*Correspondence: shaguftakhan17@rediffmail.com, Phone: +07152-240284, ORCID-ID: orcid.org/0000-0002-2827-7939

Received: 02.05.2021, Accepted: 17.09.2021

©Turk J Pharm Sci, Published by Galenos Publishing House.

lymphatic absorption, and improve solubility as well as bioavailability.⁷ Hu et al.⁸ prepared lapatinib ditosylate solid dispersions (SDs) using solvent rotary evaporation and hot melt extrusion for solubility and dissolution enhancement. SDs prepared by rotary evaporation showed 29 folds enhancement of solubility of lapatinib ditosylate compared with SDs prepared by hot-melt extrusion.

AS, an antiretroviral drug belongs to the BCS class II. Because of poor solubility and dissolution rate, it has poor oral bioavailability (60–68%) (accessed 12 Jan 2018) <https://www.drugbank.ca/drugs/DB01072>. Atazanavir is an azapeptide HIV-1 protease inhibitor that prevents the formation of mature virions through the selective inhibition of viral Gag and Gag-Pol polyprotein processing in HIV-1-infected cells.⁹ Because of its promising effect, atazanavir is the drug of choice for resisting HIV infection. However, its therapeutic efficacy is low on oral administration because of its poor bioavailability. Polymeric NPs provide a high surface area and can reduce the crystallinity, therefore, can improve the solubility of the poorly water-soluble drugs. In a study, atazanavir was loaded on eudragit RL -100 NPs to improve its oral bioavailability.¹⁰

In this investigation, gamma-cyclodextrin (γ -CD) is used to prepare NPs because atazanavir sulfate (AS) is a moderately large molecular weight drug (802.93 Da), for which the cavity size of γ -CD would be appropriate (accessed 12 Jan 2018) <https://www.drugbank.ca/salts/DBSALT000426>.

Wang et al.¹¹ prepared an inclusion complex of nystatin with γ -CD, which sufficiently increased the water solubility and storage stability of nystatin. In addition to solubility enhancement, crosslinked NPs would sustain the atazanavir release, which could reduce the gastrointestinal side effects caused by its immediate release in the stomach. Bristol Myers Squibb Company, Princeton, NJ 08543, USA. Reyataz product information (accessed April 30, 2021). Available from the following: https://packageinserts.bms.com/pi/pi_reyataz.pdf.

MATERIALS AND METHODS

Material

AS was obtained as a gift from Acebright (India) Pharma Pvt. Ltd., Bangalore, γ -CD was gifted by Wacker Chemie AG. Ashland Inc., USA, dimethyl carbonate (DMC), dimethyl formamide (DMF), and potassium chloride were supplied by LOBA Chemie, Pvt. Ltd., Mumbai India. All other chemicals used in this study were of analytical grade and obtained from LOBA Chemie, Pvt. Ltd., Mumbai.

Preparation of ASNPs

The ASNPs were prepared by the crosslinking method. Varying amounts of γ -CD and AS were dissolved in 30 mL DMF. To the solution, 1 mL triethylamine followed by 15 mL DMC was added and refluxed at 80°C for 3 h to allow the reaction to occur. The reaction mixture was allowed to cool and the formed NPs were separated by centrifugation at 10,000 rpm (Model C-24BL, Remi Motors Ltd, Mumbai, India) and freeze-dried.¹²

Saturation solubility determination

An excess amount of ASNPs was added to 10 mL of water/acid buffer pH 1.2 or phosphate buffer pH 6.8 in the amber-colored vials and kept under stirring for 48 h at 25 ± 0.5°C. The resultant suspensions were then centrifuged at 10,000 rpm and supernatants were analyzed at 279 nm (λ_{max} of AS in water and phosphate buffer) for water and phosphate buffer pH 6.8 and at 246 nm (λ_{max} of AS in acid buffer) for acid buffer pH 1.2 respectively (model UV 2401 PC, Shimadzu Corporation, Kyoto, Japan).

The results were compared to the saturation solubility of AS in water, acid buffer pH 1.2, and phosphate buffer pH 6.8 respectively and the solubility enhancement ratio was calculated.^{13–15}

Characterization of ASNPs

Determination of drug loading capacity and percent entrapment efficacy (EE)

100 mg ASNPs was stirred in 100 mL of acid buffer pH 1.2 for 48 h, centrifuged and the supernatant was analyzed at 246 nm for AS.^{16,17}

Drug-loading capacity and percent EE were calculated according to the following equations:

$$\text{Drug loading capacity} = \frac{\text{weight of drug entrapped in nanoparticles}}{\text{total weight of drug}} \times 100 \quad (1)$$

$$\% \text{Encapsulation efficiency} = \frac{\text{Actual drug content in nanoparticles}}{\text{Theoretical drug content}} \times 100 \quad (2)$$

Determination of particle size and zeta potential

The particle size, polydispersity index, and zeta potential of ASNPs were determined using Zetasizer (model-ZS90, Malvern Instrument Ltd., Worcestershire, UK) after appropriate dilution.^{10,18}

Solid state characterization

Solid-state characterization by fourier transformed infrared spectroscopy (FTIR), differential scanning calorimetry (DSC) and X-ray powder diffraction (XRPD)

FT spectroscopy was done to check the changes in drug upon NP formation. AS, γ -CD, physical mixture of AS and γ -CD, and ASNPs were compressed with a small quantity of KBr and scanned between 4000 and 400 cm^{-1} (model-8400S, Shimadzu Asia Pacific Pvt. Ltd., Singapore) (Figure 1).¹⁹

For DSC, AS, γ -CD, physical mixture of AS and γ -CD and ASNPs were scanned between 30 and 300°C with the temperature rise at the rate of 10°C/min under the nitrogen environment (model- DSC 620, DSC Seiko nanotechnology, country) (Figure 2).^{20,21}

XRPD of these samples was performed at a voltage of 40 kV and 30 mA with a scanning rate of 2°C/min (model- XRD-7000, Shimadzu, Japan) (Figure 3).^{22,23}

Surface morphology study using scanning electron microscopy (SEM)

The surface morphology of ASNPs was probed to examine the surface characteristics of particles. ASNPs were diluted and an aliquot of the diluted preparation was dried. The dried ASNPs were mounted on the double-sided conductive metallic stud. The sample was then coated by ion coating with platinum by

sputter coater for 40 sec in the vacuum at a current intensity of 40 mA. The sample was viewed by SEM (model-S-3700N, Hitachi, Japan) using a secondary electron detector with an accelerating voltage of 15 kV and a working distance of 2 mm. Images of SEM were digitally captured using Quartz PCI digital imaging software (Quartz Imaging Corporation, British Columbia, Canada) (Figure 4).²⁴⁻²⁶

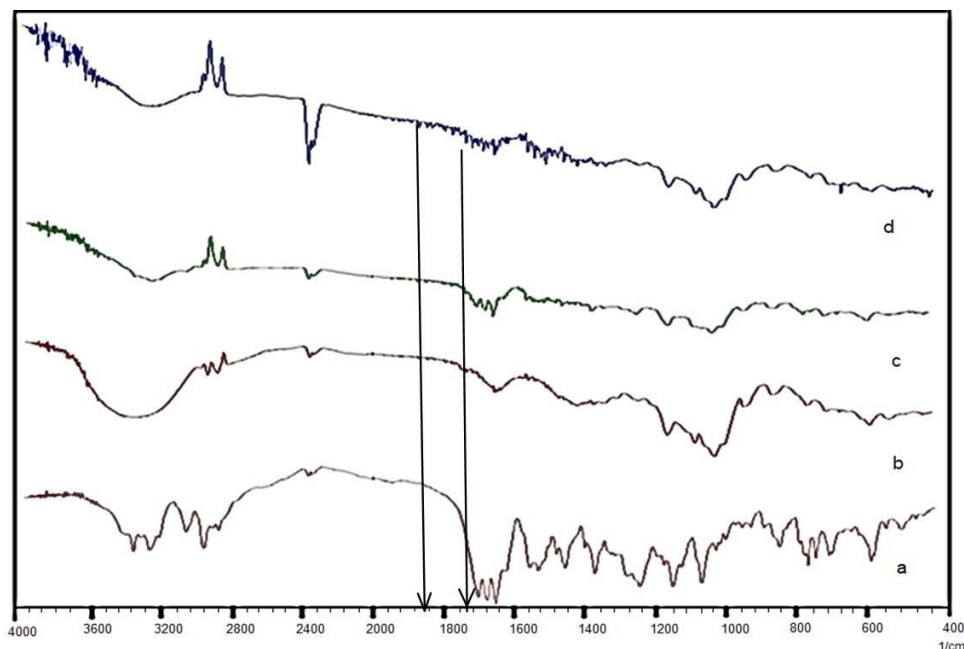


Figure 1. FTIR of a) AS; b) γ -CD; c) Physical mixture of atazanavir sulfate and γ -CD; d) ASNPs

FTIR: Fourier transformed infrared spectroscopy, γ -CD: Gamma-cyclodextrin, ASNPs: Atazanavir sulfate-loaded nanoparticles

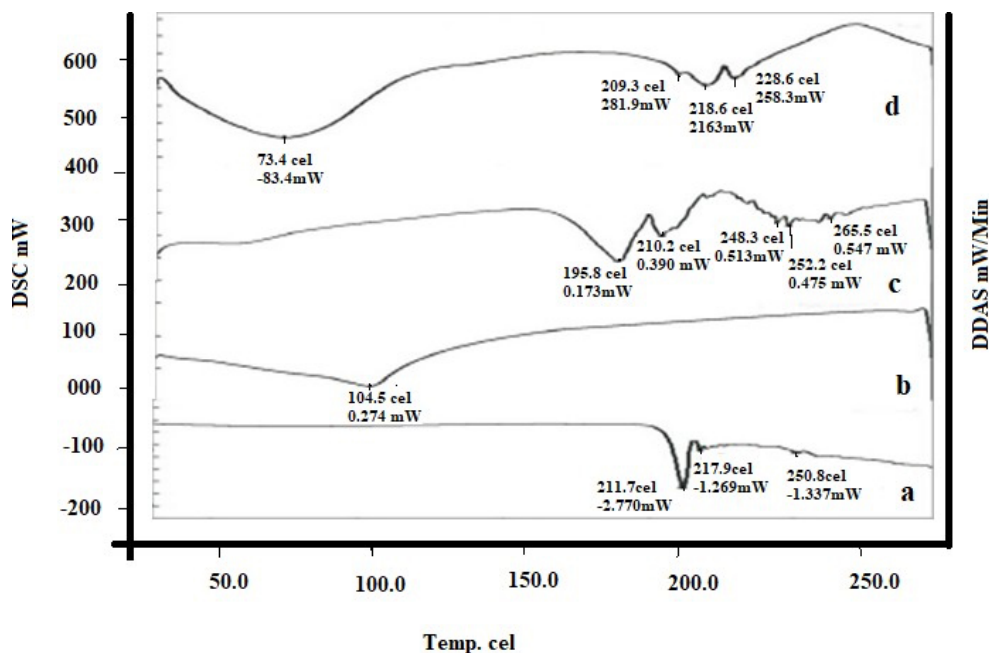


Figure 2. DSC thermogram of a) AS; b) γ -CD; c) Physical mixture of atazanavir sulfate and γ -CD; d) ASNPs

DSC: Differential scanning calorimetry, γ -CD: Gamma-cyclodextrin, ASNPs: Atazanavir sulfate-loaded nanoparticles

In vitro release studies

To elucidate the effect of different dissolution media on the drug release, *in vitro* dissolution testing of ASNPs was performed for 12 h in water, acid buffer pH 1.2, and phosphate buffer pH 6.8 using the dialysis method. NPs equivalent to 15 mg of AS were placed in an activated cellulose dialysis bag containing 2 mL of the dissolution medium, which was sealed from both ends. The dialysis bag was then suspended through the shaft of the USP apparatus (type I), from which the basket was removed into the jar containing 900 mL dissolution medium maintained at $37 \pm 0.5^\circ\text{C}$ under stirring at 100 rpm. Samples were withdrawn at the pre-determined intervals and analyzed at 279 nm for water and phosphate buffer, and 246 nm for the acid buffer, respectively.^{27,28}

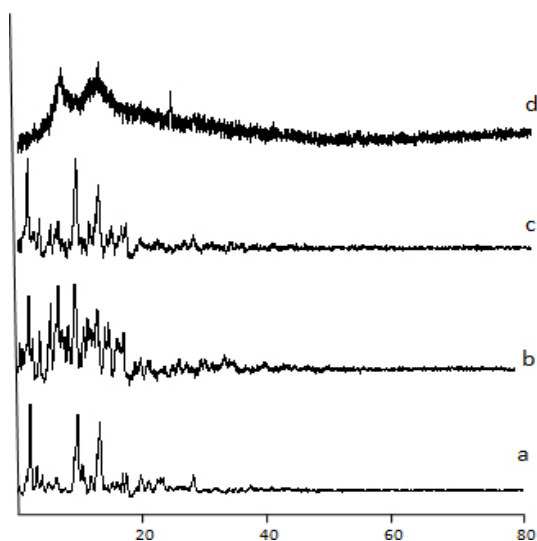


Figure 3. XRD diffractogram of a) Atazanavir sulfate; b) γ -CD; c) Physical mixture of atazanavir sulfate and γ -CD; d) Batch F5 of ASNPs

XRD: X-ray diffraction, γ -CD: Gamma-cyclodextrin, ASNPs: Atazanavir sulfate-loaded nanoparticles

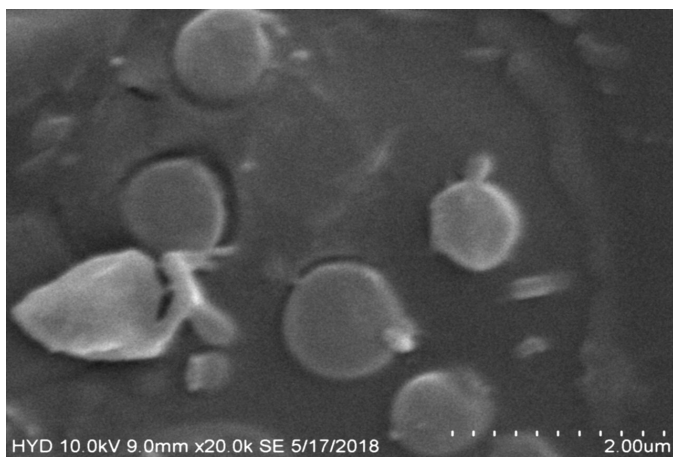


Figure 4. SEM image of batch (F5) of ASNPs

SEM: Scanning electron microscopy, ASNPs: Atazanavir sulfate-loaded nanoparticles

ASNPs wrapped in aluminum foil were placed at $25 \pm 2^\circ\text{C}$ and $60 \pm 5\%$ RH for 6 months in the stability chamber (model- HTC-3003, Wadegati™ Labe Quip (P) Ltd., Andheri (E), Mumbai, India). Every month, ASNPs were analyzed for physical changes, drug-loading capacity, particle size, and zeta potential.¹⁰

Statistical analysis

Comparison was done by ANOVA followed by Bartlett's test using Graph Pad Prism 7.0. $p < 0.5$ was considered to be significant difference between groups.

RESULTS AND DISCUSSION

Formulation of ASNPs

ASNPs were successfully obtained by the crosslinking method. NPs were prepared by varying the ratios of drug: γ -CD and by varying the concentrations of drug and γ -CD at a constant volume of DMC.

Cross-linked CD was obtained by reacting CD with a carbonyl compound DMC. The reaction is essentially performed out with an excessive carbonyl compound, in the polar aprotic solvent DMF. The presence of an absorption band between 1750 cm^{-1} to 1860 cm^{-1} in the FTIR of ASNPs as marked by the arrows in the Figure 1d, is due to the carbonyl (C=O) group. The absence of this absorption band in the FTIR of the physical mixture (Figure 1c) confirms the successful cross-linked CD network formation in the NPs.

Evaluation of polymeric nanoparticles

Drug-loading capacity and % EE

As shown in Table 1, drug-loading capacity of ASNPs (batches F1 to F9) ranged from 6.73 ± 0.3 to $37.98 \pm 0.4\%$, while percentage EE was between 14.38 ± 0.2 and $75.97 \pm 0.3\%$. Formulation F5 prepared from the 1:1 ratio of AS and γ -CD at 10 mg/mL concentration had the maximum drug-loading capacity (37.98 ± 0.4) and % EE (75.97 ± 0.3). With the increase in drug and polymer concentration up to 10 mg/mL and their ratio 1:1, both drug loading capacity, and % EE increased, possibly because of the compact crosslinked network formation. Maximum drug-loading was obtained at 10 mg/mL γ -CD because at this concentration, the number of OH groups of γ -CD to be crosslinked with DMC to form CD-C-O bond would be optimum, however, at lower γ -CD concentrations than this. Availability of OH groups to participate in crosslinking would be insufficient causing loose network formation and low EE. Higher entrapment in densely crosslinked NPs suggests entrapment of AS both within CD cavity and between the crosslinked network. Similar findings were reported by Singh et al.²⁹ at higher γ -CD than 10 mg/mL, DMC becomes insufficient to crosslink the available OH groups, forming a weak network with consequent low EE.

Particle size and zeta potential

The average particle size of ASNPs (batch F1 to F9) was between $65.4 \pm 1.3\text{ nm}$ and $439.6 \pm 2.2\text{ nm}$ as shown in Table 1. It could be noted that the particle size was influenced by the concentration of γ -CD. At higher levels of γ -CD, there was a greater viscosity increase after reflux, ensuing bigger particles.

ASNPs displayed positive zeta potential in the range 20.6 ± 0.2 mV to 41.0 ± 0.3 mV. The zeta potential of batch F5 was 40.3 ± 0.3 mV representing excellent stability of NPs. A high zeta potential was sufficient to keep particles separate from each other due to electrostatic repulsion. A positive zeta potential was due to the basic nature of AS. Polydispersity index of ASNPs in the range from 0.162 ± 0.02 to 0.439 ± 0.01 shows good homogeneity.

Solid state characterization

FTIR, DSC, and XRD

The FTIR spectrum of AS showed a sharp peak at 3313.48 cm^{-1} due to NH stretching, 2873.74 cm^{-1} due to CH stretching, 1701.10 cm^{-1} due to C=O stretching, 1515.94 cm^{-1} due to C=C stretching, 1242.07 cm^{-1} due to S=O stretching and 1124.42 cm^{-1} due to CN stretching (Figure 1a). All the bands were found intact in the FTIR spectrum of the physical mixture of AS and γ -CD indicating no interaction of the drug with the polymer. FTIR of ASNPs revealed additional absorption peaks from 1750 cm^{-1} to 1860 cm^{-1} (Figure 1d), which were absent in the spectra of both γ -CD and the physical mixture. These peaks indicated the carbonyl bonds between the γ -CD molecules.³⁰ The absence of characteristic peak of AS at 3313.48 cm^{-1} in the spectrum ASNPs indicated hydrogen bond formation between AS and hydroxyl groups of CD. Broadening of characteristic peaks of AS in the NPs suggests the formation of hydrogen bond formation between AS and CD.

The DSC thermograms of AS showed a sharp endothermic peak at 211.7°C corresponding to its melting point. AS in the current investigation is the type A polymorphic form as its DSC is similar to the DSC of AS identified by Kim et al.³¹, in which it was revealed that the melting endotherm starts at 169°C , peaks at 200°C and extends to about 225°C . In the physical mixture of drug with γ -CD, the endothermic peak of the drug was retained at 195.8°C and 210.2°C . ASNPs depicted the endothermic peak at 209°C and 218°C due to the melting of atazanavir. The thermal behavior seems similar to that one revealed by Kim et al.³¹ in their pioneering investigations on AS. Thus, AS was intact in the NPs.

XRD of AS showed characteristic sharp and intense peaks at $2\theta = 11^\circ, 13^\circ, 18^\circ, 21^\circ,$ and 34° (Figure 3a) due to its crystalline nature, while characteristic peaks of AS had completely disappeared in the NPs, which confirms the conversion of the crystalline drug into an amorphous form upon NP formation. The XRD of γ -CD (Figure 3b) showed sharp peaks up to 20° because it is crystalline, but in the NPs, its peaks were lost. This could be due to the participation of its hydroxyl groups in the crosslinking with DMC. The crosslinking leads to the formation of irregular arrangements and tortuous structure.²⁹

Surface morphology study

From the SEM images of ASNPs, it could be noted that NPs were almost spherical, uniform with a smooth surface.

Saturation solubility

The saturation solubility of AS in water, acid buffer (pH 1.2), and phosphate buffer (pH 6.8) was found to be 0.0046 ± 0.0003 mg/mL, 0.310 ± 0.008 mg/mL, and 0.0025 ± 0.0004 mg/mL respectively (Table 2). The saturation solubility of ASNPs increased from 5.13 to 11.71 folds in water, 0.99 to 1.167 folds in the acid buffer (pH 1.2), and 2.72 to 20.12 folds in the phosphate buffer (pH 6.8). With increasing concentration of γ -CD, solubility of the drug also increased. ASNPs with AS: γ -CD (1:2) showed the highest solubility compared to the combinations with a lower level of γ -CD. The change in the crystalline form to amorphous form upon NP formation with γ -CD as revealed in the XRD in addition to the formation of small-sized NPs, was responsible for the improvement in the solubility of the drug.

In vitro drug release

Percent cumulative drug release from ASNPs F1 to F9 batches is shown in Figure 5a to 5c in water, acid buffer (pH 1.2) and phosphate buffer (pH 6.8), respectively. Drug release after 12 h from ASNP batch F5 in water, acid buffer (pH 1.2), and phosphate buffer (pH 6.8) was found to be $88.55 \pm 0.3\%$, $91.23 \pm 0.2\%$, and $86.8 \pm 0.2\%$, respectively.

Batches that had a concentration of γ -CD 10 mg/mL or more were found to produce a higher dissolution rate. At these concentrations of γ -CD, when drug:CD ratio was 1:2, the

Table 1. Composition of ASNPs and their characteristics

Batches	Atazanavir sulphate (mg/mL)	Gamma cyclodextrin (mg/mL)	Ratio of drug: Polymers	%Drug- loading capacity*	% EE*	Particle size (nm)	Polydispersity index (PDI)
F1	5	2.5	1:0.5	9.62 ± 0.2	14.38 ± 0.2	65.4 ± 1.25	0.162 ± 0.01
F2	5	5	1:1	12.59 ± 0.4	25.18 ± 0.3	73.7 ± 1.5	0.185 ± 0.02
F3	5	10	1:2	6.73 ± 0.3	20.17 ± 0.7	92.5 ± 1.7	0.204 ± 0.01
F4	10	5	1:0.5	31.25 ± 0.3	46.75 ± 0.8	81.6 ± 1.3	0.283 ± 0.01
F5	10	10	1:1	37.98 ± 0.4	75.97 ± 0.3	99.7 ± 1.9	0.310 ± 0.01
F6	10	20	1:2	15.73 ± 0.3	47.16 ± 0.5	141.6 ± 1.6	0.354 ± 0.02
F7	15	7.5	1:0.5	17.75 ± 0.2	26.55 ± 0.2	104.4 ± 1.5	0.381 ± 0.01
F8	15	15	1:1	34.70 ± 0.4	69.40 ± 0.2	136.3 ± 1.3	0.407 ± 0.00
F9	15	30	1:2	19.96 ± 0.5	59.83 ± 0.4	439.6 ± 2.2	0.439 ± 0.01

*Represents mean \pm standard deviation (n: 3). EE: Entrapment efficiency, ASNPs: Atazanavir sulfate-loaded nanoparticles

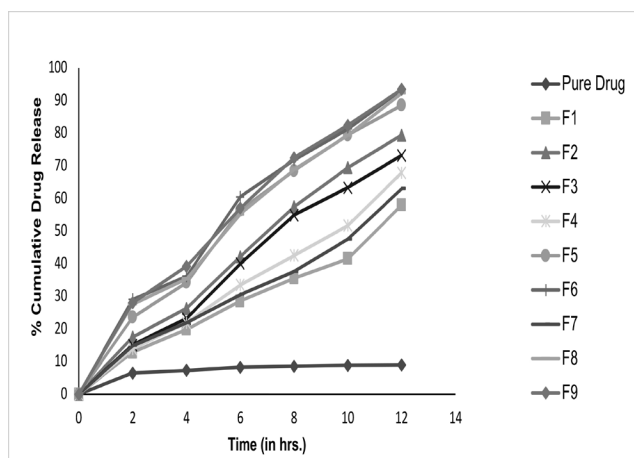


Figure 5a. *In vitro* dissolution profile of pure drug and ASNPs (batch F1 to F9) in water

ASNPs: Atazanavir sulfate-loaded nanoparticles

highest dissolution rate was found. This was because of the greater solubility increase in AS due to the greater masking of hydrophobic groups of AS within the nanochannels at this ratio.³²

Initial burst release is seen in each media, because of the rapid release of the adhered AS on the surface of NPs. The AS release rate was highest in the acid buffer, because of the basic character of AS. However, the dissolution study clearly indicates that the drug release rate in water, as well as phosphate buffer, was significantly (unpaired *t*-test, $p < 0.05$) higher than that in free AS in these media. Additionally, the drug release rate in these media is similar to the dissolution rate in the acid buffer. The dissolution profiles of batch F5 in the three dissolution media were found to be similar when compared using F2 values. For dissolution profiles in water vs. acid buffer, F2 was 57.24, in water vs. phosphate buffer, F2 was 86.01 and in acid buffer vs. phosphate buffer, F2 was 57.72, respectively. Therefore, it can be conclusively said that pH-independent drug release could be achieved from NPs although, the solubility of

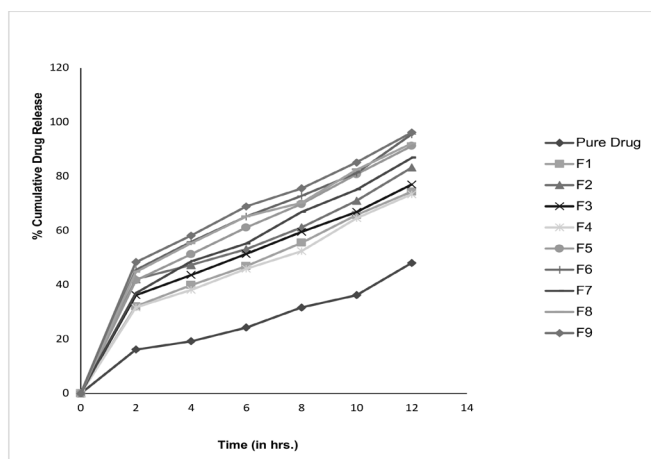


Figure 5b. *In vitro* dissolution profile of pure drug and ASNPs (batches F1 to F9) in HCl buffer (pH 1.2)

ASNPs: Atazanavir sulfate-loaded nanoparticles

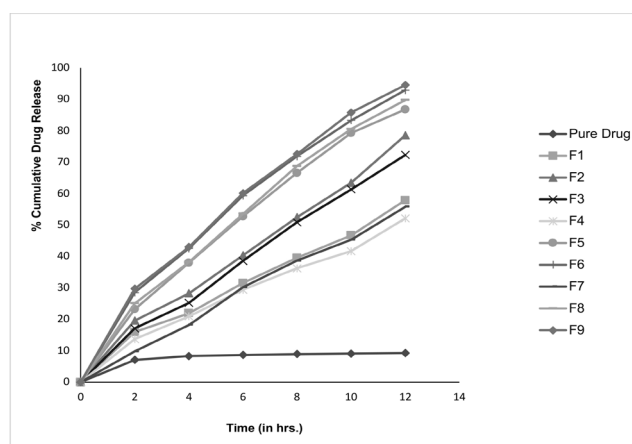


Figure 5c. *In vitro* dissolution profile of pure drug and ASNPs (batches F1 to F9) in phosphate buffer (pH 6.8)

ASNPs: Atazanavir sulfate-loaded nanoparticles

Table 2. Saturation solubility of formulations at different

Batch	Solubility (mg/mL) *		
	Water (mg/mL)	Phosphate buffer (pH 6.8) (mg/mL)	HCl buffer (pH 1.2) (mg/mL)
Pure drug	0.0046 ± 0.0003	0.0025 ± 0.0004	0.310 ± 0.008
F1	0.0236 ± 0.0006	0.0068 ± 0.0006	0.308 ± 0.007
F2	0.0256 ± 0.0005	0.0083 ± 0.0005	0.314 ± 0.006
F3	0.0277 ± 0.0007	0.0095 ± 0.0005	0.319 ± 0.005
F4	0.0289 ± 0.0003	0.0106 ± 0.001	0.340 ± 0.009
F5	0.0365 ± 0.001	0.0253 ± 0.0007	0.351 ± 0.004
F6	0.0539 ± 0.0008	0.0503 ± 0.0006	0.362 ± 0.005
F7	0.0241 ± 0.0004	0.0092 ± 0.0004	0.324 ± 0.008
F8	0.0316 ± 0.0008	0.0121 ± 0.0006	0.349 ± 0.006
F9	0.0347 ± 0.0007	0.0184 ± 0.0007	0.357 ± 0.002

*Represents mean ± standard deviation (n: 3)

free AS is higher in the acidic condition. This could be achieved because of the solubility enhancing capability of γ -CD NPs irrespective of the medium. A uniform sustained release over 12 h by the ASNPs can be a viable way to reduce side effects associated with the immediate release of AS.

Stability study

Batch F5 with the highest drug loading capacity and EE with high zeta potential and considerable homogeneity and small size were considered optimum and kept for stability testing for 6 months at $25 \pm 2^\circ\text{C}$ and $60 \pm 5\%$ RH. The batch showed insignificant differences in the drug content ($p = 0.73$), % EE ($p = 0.77$), particle size ($p = 0.53$), zeta potential ($p = 0.52$) and *in vitro* drug release ($p > 0.5$), when analyzed by ANOVA followed by Bartlett's test using Graph Pad Prism 7.0.

CONCLUSION

AS-loaded polymeric NPs were successfully prepared using the crosslinking method. γ -CD was found to be effective in entrapping moderately large molecular weight drug AS and improving its solubility, for which other CDs could not have possibly been so successful owing to their small cavity size. The obtained NPs displayed a significant increase in the dissolution rate of AS irrespective of pH of the medium, which can be considered an important achievement for overcoming its dissolution rate-limited poor bioavailability. Additionally, as the NPs could sustain the drug release so can alleviate the side effects associated with the AS immediate release. As similar dissolution profiles were obtained in each medium, there is no need to design a gastroretentive formulation of AS, as uniform drug release throughout the GIT over prolonged periods is possible with the prepared NPs in this investigation.

Nevertheless, further *in vivo* studies in animals and humans should be conducted to support the results obtained in this investigation.

Ethics

Ethics Committee Approval: Not required.

Informed Consent: Not required.

Peer-review: Externally peer-reviewed.

Authorship Contributions

Concept: S.A.Q.K., Design: S.A.Q.K., Data Collection or Processing: D.D., Analysis, or Interpretation: S.A.Q.K., Literature Search: D.S., Writing: M.U., B.R., S.A.Q.K.

Conflict of Interest: No conflict of interest was declared by the authors.

Financial Disclosure: The authors declared that this study received no financial support.

REFERENCES

1. Yellela SRK. Pharmaceutical technologies for enhancing oral bioavailability of poorly soluble drugs. *J Bioequivalence Bioavailab.* 2010;2:28-36.
2. Sharma D, Soni M, Kumar S, Gupta GD. Solubility enhancement - eminent role in poorly soluble drugs. *Research J Pharm Tech.* 2009;2:220-224.
3. Kumar A, Sahoo SK, Padhee K, Kochar PPS, Sathapathy A, Pathak N. Review on solubility enhancement techniques for hydrophobic drugs. *Pharm Glob.* 2011;3:1-7.
4. Fahr A, Liu X. Drug delivery strategies for poorly water-soluble drugs. *Expert Opin Drug Deliv.* 2007;4:403-416.
5. Gomez-Orellana I. Strategies to improve oral drug bioavailability. *Expert Opin Drug Deliv.* 2005;2:419-433.
6. Boudad H, Legrand P, Lebas G, Cheron M, Duchêne D, Ponchel G. Combined hydroxypropyl-beta-cyclodextrin and poly(alkylcyanoacrylate) nanoparticles intended for oral administration of saquinavir. *Int J Pharm.* 2001;218:113-124.
7. Sawant KK, Parmar B, Mandal SA, Petkar KC, Patel LD. Valsartan loaded solid lipid nanoparticles: development, characterization and *in vitro* and *ex vivo* evaluation. *Int J Pharm Sci Nanotech.* 2011;4:1483-1490.
8. Hu XY, Lou H, Hageman MJ. Preparation of lapatinib ditosylate solid dispersions using solvent rotary evaporation and hot melt extrusion for solubility and dissolution enhancement. *Int J Pharm.* 2018;552:154-163.
9. Robinson BS, Riccardi KA, Gong YF, Guo Q, Stock DA, Blair WS, Terry BJ, Deminie CA, Djang F, Colonna RJ, Lin PF. BMS-232632, a highly potent human immunodeficiency virus protease inhibitor that can be used in combination with other available antiretroviral agents. *Antimicrob Agents Chemother.* 2000;44:2093-2099.
10. Singh G, Pai RS. Atazanavir-loaded eudragit RL 100 nanoparticles to improve oral bioavailability: optimization and *in vitro/in vivo* appraisal. *Drug Deliv.* 2016;23:532-539.
11. Wang J, Jin Z, Xu X. Gamma-cyclodextrin on enhancement of water solubility and store stability of nystatin. *J Incl Phenom Macrocyclic Chem.* 2014;78:145-150.
12. Trotta F, Tumiatti W. Cross-linked polymers based on cyclodextrins for removing polluting agents. Available from: <https://patentimages.storage.googleapis.com/da/b1/47/521f420ce02a27/US20050154198A1.pdf>
13. Wilson B, Samanta MK, Santhi K, Kumar KP, Paramakrishnan N, Suresh B. Poly(*n*-butylcyanoacrylate) nanoparticles coated with polysorbate 80 for the targeted delivery of rivastigmine into the brain to treat Alzheimer's disease. *Brain Res.* 2008;1200:159-168.
14. Wuyts B, Brouwers J, Mols R, Tack J, Annaert P, Augustijns P. Solubility profiling of HIV protease inhibitors in human intestinal fluids. *J Pharm Sci.* 2013;102:3800-3807.
15. Berlin M, Ruff A, Kesiosoglou F, Xu W, Wang MH, Dressman JB. Advances and challenges in PBPK modeling-analysis of factors contributing to the oral absorption of atazanavir, a poorly soluble weak base. *Eur J Pharm Biopharm.* 2015;93:267-280.
16. Belgamwar A, Khan S, Yeole P. Intranasal chitosan-g-HP-CD nanoparticles of efavirenz for the CNS targeting. *Artif Cells Nanomed Biotechnol.* 2018;46:374-386.
17. Yadav SK, Mishra S, Mishra B. Eudragit-based nanosuspension of poorly water-soluble drug: formulation and *in vitro-in vivo* evaluation. *AAPS PharmSciTech.* 2012;13:1031-1044.
18. Ahmad N, Alam MA, Ahmad R, Naqvi AA, Ahmad FJ. Preparation and characterization of surface-modified PLGA-polymeric nanoparticles used to target treatment of intestinal cancer. *Artif Cells Nanomed Biotechnol.* 2018;46:432-446. Retraction in: *Artif Cells Nanomed Biotechnol.* 2020;48:1328.

19. Sahu PL. Indian Pharmacopoeia. The Indian Pharmacopoeia Commission. 2018. Available from: <https://www.idma-assn.org/pdf/dr-pl-sahu.pdf>
20. Çirpanlı Y, Bilensoy E, Doğan AL, Çaliş S. Comparative evaluation of polymeric and amphiphilic cyclodextrin nanoparticles for effective camptothecin delivery. *Eur J Pharm Biopharm.* 2009;73:82-89.
21. Mu L, Feng SS. A novel controlled release formulation for the anticancer drug paclitaxel (Taxol): PLGA nanoparticles containing vitamin E TPGS. *J Control Release.* 2003;86:33-48.
22. Sun SB, Liu P, Shao FM, Miao QL. Formulation and evaluation of PLGA nanoparticles loaded capecitabine for prostate cancer. *Int J Clin Exp Med.* 2015;8:19670-19681.
23. Shaikh J, Ankola DD, Beniwal V, Singh D, Kumar MN. Nanoparticle encapsulation improves oral bioavailability of curcumin by at least 9-fold when compared to curcumin administered with piperine as absorption enhancer. *Eur J Pharm Sci.* 2009;37:223-230.
24. Win KY, Feng SS. Effects of particle size and surface coating on cellular uptake of polymeric nanoparticles for oral delivery of anticancer drugs. *Biomaterials.* 2005;26:2713-2722.
25. Merisko-Liversidge E, Sarpotdar P, Bruno J, Hajj S, Wei L, Peltier N, Rake J, Shaw JM, Pugh S, Polin L, Jones J, Corbett T, Cooper E, Liversidge GG. Formulation and antitumor activity evaluation of nanocrystalline suspensions of poorly soluble anticancer drugs. *Pharm Res.* 1996;13:272-278.
26. Chattopadhyay N, Zastre J, Wong HL, Wu XY, Bendayan R. Solid lipid nanoparticles enhance the delivery of the HIV protease inhibitor, atazanavir, by a human brain endothelial cell line. *Pharm Res.* 2008;25:2262-2271.
27. Abouelmagd SA, Sun B, Chang AC, Ku YJ, Yeo Y. Release kinetics study of poorly water-soluble drugs from nanoparticles: are we doing it right? *Mol Pharm.* 2015;12:997-1003.
28. Wilson B, Samanta MK, Santhi K, Kumar KP, Ramasamy M, Suresh B. Chitosan nanoparticles as a new delivery system for the anti-Alzheimer drug tacrine. *Nanomedicine.* 2010;6:144-152.
29. Singh V, Xu J, Wu L, Guo T, Guo Z, York P, Gref R, Zhang J. Ordered and disordered cyclodextrin nanosponges with diverse physicochemical properties. *RSC Adv.* 2017;7:23759-23764.
30. Rao MR, Bhingole RC. Nanosponge-based pediatric-controlled release dry suspension of gabapentin for reconstitution. *Drug Dev Ind Pharm.* 2015;41:2029-2036.
31. Kim S, Lotz BT, Malley MF, Gougoutas JZ, Davidovich M, Srivastava SK. Process for preparing atazanavir bisulfate and novel forms. US Patent. 2005; US 20050256202A1.
32. Ansari KA, Vavia PR, Trotta F, Cavalli R. Cyclodextrin-based nanosponges for delivery of resveratrol: *in vitro* characterisation, stability, cytotoxicity and permeation study. *AAPS PharmSciTech.* 2011;12:279-286.